

Comparing the Adhesion Capability of Periodontal Ligament Fibroblast Cells to Nano-hydroxyapatite Silicate-Based Cement and Silicate-Based Cement Alone

Hooman Khorshidi¹, Shahab Honar¹, Saeed Raoofi¹, Negar Azarpira²

¹Department of Periodontics, School of Dentistry, Shiraz University of Medical Sciences, Shiraz, Iran

²Department of pathology, school of medicine, Shiraz University of Medical Sciences, Shiraz, Iran

Received 11 February 2021 and Accepted 12 March 2021

Abstract

Introduction: Silicate-based cement alone and Hydroxyapatite as bone filling materials lead to successful results in implant dentistry and regenerative medicine. The purpose of this study was to compare the adhesion capability of periodontal ligament fibroblast cells (PDLFC) to the Nanohydroxyapatite silicate-based cement and silicate-based cement alone in vitro.

Methods: Primary cell cultures of PDLFCs were obtained from clinically healthy third molars teeth. These third molars were either extracted for orthodontic reasons or extracted due to the impaction of teeth. Cells subcultured at a density of 10000 cells/well in 24-well plates. Methyl-tetrazolium bromide (MTT) assay was performed to evaluate the survival and proliferation of fibroblasts on 24h, 72h, and 1 week after the cell culture. Scanning Electron Microscopy (SEM) analysis was used to examine the morphology of PDLFCs on the two scaffolds. **Results:** Cells were found growing in close proximity to both minerals but in terms of fibroblast cell attachment. Adding Nanohydroxyapatite did not improve cellular proliferation and silicate-based cement alone showed superior cellular proliferation in 72 hours. After 24h and 1 week both minerals showed the same response.

Conclusion: Although both Nanohydroxyapatite silicate-based cement and silicate-based cement alone are biocompatible, but nanohydroxyapatite silicate-based cement did not show improved biological activities when compared with silicate-based cement.

Keywords: Apc cement; Bioceramics; Cell proliferation; Nanobiomaterials; Regeneration

KhorshidiH, HonarSH, RaoofiS, zarpiraN. Comparing the Adhesion Capability of Periodontal Ligament Fibroblast Cells to Nano-hydroxyapatite Silicate-Based Cement and Silicate-Based Cement Alone. *J Dent Mater Tech* 2021; 10(2): 79-86.

Introduction

Hydraulic silicate cements have the ability of apatite core formation and can stimulate tissue repair, osteogenesis, and cementogenesis(1–3). Silicate-based cement alone enjoys good handling, which is a critical feature as a bone substitute material (4). Another material with successful results in implant dentistry and regenerative processes is Hydroxyapatite (HA). HA, in the form of powder, has low clinical handling capability; however, due to its excellent compatibility with hard and soft tissue, it is an ideal material for implant dentistry. Recently, many studies have been carried out on the form of Nano hydroxyapatite (4, 5–10). A Nano-sized hydroxyapatite (less than 100 nanometers in size) is ideal because it can stimulate inorganic phase in the bone (11, 12); on the other hand, HA Nanoparticles with an increased ratio of surface to volume may cause an increase in cell adhesion, proliferation, and osteoblast adhesion (8, 13). In a recent study, the effect of silicate-based cement and its combination with Nano-HA has been evaluated on implant primary stability and it was concluded that both cements could equally increase primary stability (4).

The aim of this study was to compare the adhesion capability of periodontal ligament fibroblast cells to the Nanohydroxyapatite silicate-based cement and silicate-based cement alone in vitro. In addition, the cellular proliferation and attachment of PDLFCs to test materials were examined to observe the physical properties of the cells following adding Nanohydroxyapatite particles.

Periodontal ligament fibroblast cells culture

Ten third molar teeth (extracted from healthy subjects due to non-pathological problems) were collected and placed in a basic medium [α -MEM (Minimum Essential Medium α) supplemented with 10% FBS (fetal bovine serum)]. The samples were transferred to the laboratory at 4 ° C. The PDL tissue separation was performed under sterile conditions, within a biohazard laminar flow hood for each tooth. Tooth surfaces were first cleaned with 70% ethanol. A scalpel blade was used to remove PDL from the root surface. Tissue was cut into small pieces (smaller than 0.5 mm) and cultured in cell culture plates in DMEM containing 10% fetal bovine serum and 0.5% antibiotics (diluted from a stock solution containing 5000 U/ml penicillin and 5000 U/ml streptomycin) at 37° C in an atmosphere of 100% humidity and 5% CO₂. The cells that grew were detached from the culture flask using 0.05% (w/v) trypsin and 0.05 mM (w/v) EDTA and transferred to 24-well-plates where they were subcultured at a density of 10000 cells/well.

2.2. Cell suspension and Counting

The 0.5 ml of cell suspension was taken using a sterile pipette and placed in an Eppendorf tube. 100 μ L of cells were transferred to another Eppendorf tube and 400 μ L of Trypan Blue 0.4% was added and slowly mixed.

Pipettes were used to obtain 100 μ L of trypan blue treated cell suspension and applied to a homocytometer. The microscope was used to focus on homocytometer grid lines with a 10-fold objective. Live cells (Live cells do not stain with Trypan Blue) were counted in a set of 16 squares.

For determining the number of cells/ml and the total number of cells the following formula was used:

$$cell/ml = \frac{\# \text{ of cells counted}}{\# \text{ squares counted}} \times 10000 \times \frac{1}{(\text{dilution factor})}$$

Total # cells = cells/ml \times vol. of original cell suspension

To calculate the percentage of viable cells the following formula was used:

$$\%viability = \frac{\#viable \text{ cells counted}}{\text{Total \# cells counted}} \times 100$$

Experimental design

In this study we had 3 groups: Group 1 Silicate-Based Cement alone (APC): 90% Portland cement type 1 (Fars Cement Co, Iran) with 10% Calcium Chloride (Kimia Material Co, Iran) additive - using a volumetric spoon. Group 2 Nanohydroxyapatite silicate-based cement (APC +Nano-HA): Based on previous experience (4), the ratio of the two materials was set to 25% APC in combination with 75% Nanohydroxyapatite (PardisPajouheshFanavaran Yazd, Iran) - using the volumetric spoon. Group 3 Control: PDLFCs seeding on a culture plate (as control). Each test group materials mixed with distilled water for setting reaction. APC was mixed with water at a 2: 1 ratio; APC +Nano-HA was mixed with water at a 3: 1 ratio. Scanning electron microscopy by a TESCAN scanning electron microscope (VEGA 3 – TESCAN, Czech Republic) at $\times 5k$ magnification was used to evaluate the surface morphology. Zeiss EM10C transmission electron microscope (TEM) at 80 kV (Zeiss, Germany) was performed to obtain the morphology and size of the nanoparticles.

The mixed test materials placed into 48-well plates (8-well plates for each material for 3 timing periods of 24h, 72h and 1 week). Each experiment was done triplicate.

MTT assay was used to evaluate the survival and proliferation of fibroblasts on days 24, 72 and 1 week after cell culturing. A fresh culture medium with 10% MTT was added to each well, and the plates at 37 ° C Incubated for 4 hours. The culture medium of each well was extracted and replaced with dimethyl sulfoxide solvent. Then, 100 μ l of each purple solution was transferred to a 96-well Elisa reader plate. The absorbance of the dye was measured by Elisa reader (POLARstar Omega, Germany) at 570 and 630 nm. Optical density (OD, absorbance) of wells was used to calculate the percentage of survival of cells in each experimental group relative to the control group.

$$\text{Cell Survival} = \text{OD Test} / \text{OD control} * 100$$

The morphology of PDLFC in two scaffolds was examined by scanning electron microscopy (S-750, Hitachi, and Tokyo, Japan), then PDLFCs were seeded in each scaffold in 24 well plastic culture plates. Forty-eight hours after initial seeding, the culture medium was discarded and cells were washed slowly with a solution containing phosphate three times. Cells were fixed on scaffolds with 2.5% glutaraldehyde for 12 hours. The fixative removed and the scaffolds were carefully washed with phosphate-buffered solution.

Then the scaffolds were exposed for 15 minutes to sequential dehydration with a series of ethanol (50%, 70%, 80%, 90% and 95%). The isoamyl acetate replaced

and the scaffolds were allowed to dry at a typical critical point, then coated with gold using an ion-sputtering coater (IB-5, Eiko, Japan) and subjected to a scanning electron microscope for evaluation of cell attachment and morphology.

Data analysis

In the MTT analysis, mean values and standard deviation were calculated for each group. Differences for each material between the three-time periods tested according to the analysis of variance (ANOVA) and one-way analysis of variance were also performed for the material with significant difference by ANOVA. Differences between the two substances for each time period were assessed using Student-t test. The significance level was considered to be 0.05.

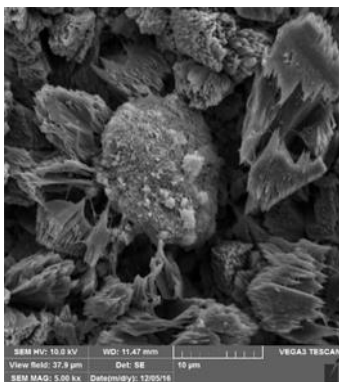


Figure 1. SEM image of APC+nano-HA substrate. Note the needle-like Hydroxyapatite crystals

Result

Table I shows MTT data analysis and statistics of two different substrate (APC&APC+nano-HA) for 24, 72 h, and 1 week. In terms of cell population, data analysis of MTT assay reflects no statistically significant difference between APC & APC+nano-HA groups at 24 h and 1 week ($P = 0.511$ & 0.162 respectively). Although there is a significant difference between APC & APC+nano-HA groups at 72 h for the benefit of the APC group ($p=0.016$).

Fig. 3 shows the cell number on the APC substrates determined by the MTT assay 24, 72 h, and 1 w after

This study was carried out in accordance with the guidelines of the Declaration of Helsinki as revised in Edinburgh (1975). The study protocol was approved by the vice chancellery for research affairs of Shiraz University of Medical Sciences, Shiraz, Iran (code: 95-01-03-11625 and 10018). A written and verbally informed consent was obtained from all participants.3. Results

SEM for Surface characteristics

APC + nanoHA surfaces showed irregular mixed surface features including round and/or sharp and cuboidal crystals. (Figure 1)

Imaging Transmission Electron Microscope (TEM) of hydroxyapatite nanoparticles by means of fast electron presented in figure 2. The size of nanoparticles is about 20-25 nanometers.

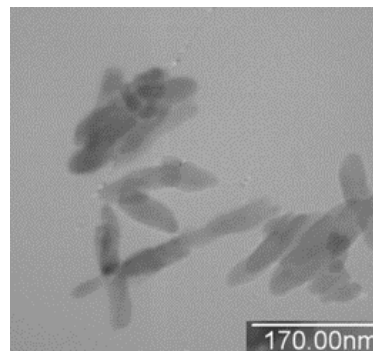


Figure 2. Transmission Electron Microscopy (TEM) of Hydroxyapatite Nanoparticles

seeding. The cell population after 24 h reflects initial adhesion on the APC substrates, and the great increase in the population after 72 h indicates subsequent proliferation of the cells while there is a decline in cell population after 1 week to the level of the initial adhesion at 24 h. MTT data analysis shows statistically significant differences between three times .Table 1 and II. ($P = 0.001$)

On the other hand, the cell population of APC+nano- HA substrates After 24, 72 h and 1 week of seeding, reflects initial adhesion on the substrates with no statistically significant difference between three times .Table I. ($P = 0.388$).

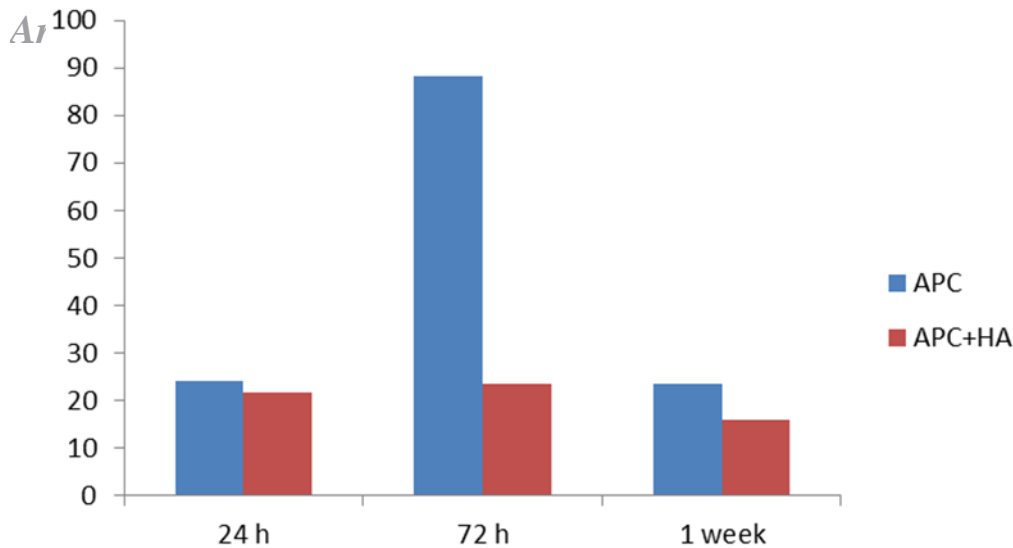


Figure 3. The number of cells on each APC & APC+ Nano-HA pellet 24 h, 72 h and 1 week after seeding determined by MTT assay.

Table I. MTT data analysis and statistics of two different substrates (APC&APC +Nano-HA) for 24, 72 h and 1 week

| Time | silicate-based cement alone(APC) | Nanohydroxyapatite silicate-based cement (APC +Nano-HA) | P value |
|---------|----------------------------------|---|---------|
| 24 h | 24.23±5.121 | 21.62±7.90 | 0.511 |
| 72 h | 72.77±34.923 | 23.61±14.38 | 0.016 |
| 1 week | 23.54±11.078 | 15.85±4.51 | 0.162 |
| P value | 0.001 | 0.388 | |

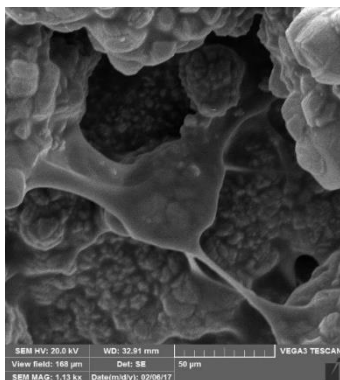
Table II. Multiple comparison analysis of different time periods of seeding

| APC(silicate-based cement alone) | | |
|----------------------------------|--------|-------|
| Time | | Sig. |
| 24 h | 72h | 0.042 |
| | 1 week | 0.989 |
| 72h | 24h | 0.042 |
| | 1 week | 0.038 |
| 1 week | 24h | 0.989 |
| | 72h | 0.038 |

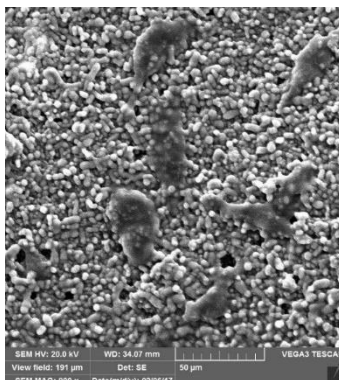
Scanning Electron Microscopy (SEM) for Cellular analysis

Fibroblast cells showed good adaptation and also showed spreading cytoplasmic extensions which are essential for

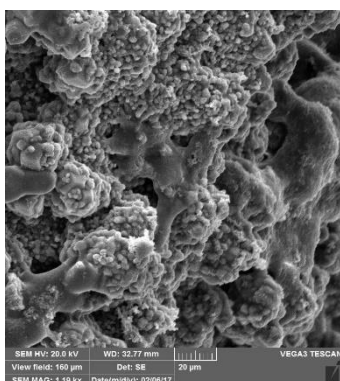
attachment and the proliferation of cells. A variety of cellular forms was observed. (Figure 4) The variety of cellular morphologies indicating the movement and proliferation of fibroblasts in the test materials.



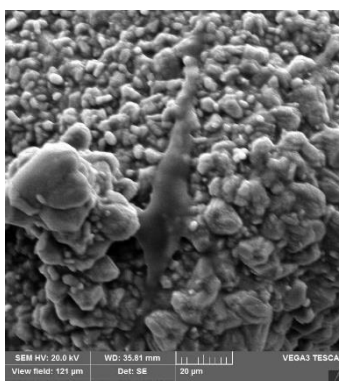
(a)



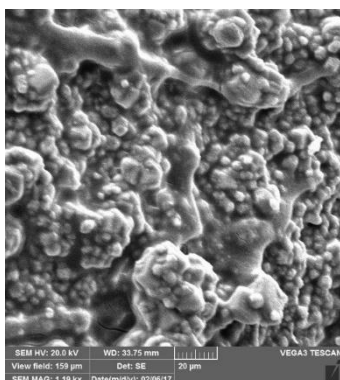
(d)



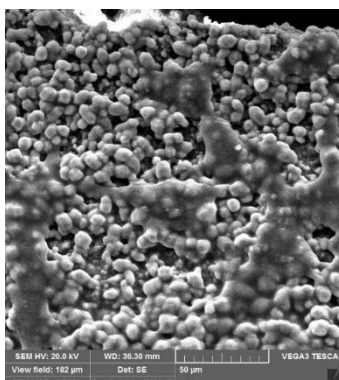
(b)



(e)



(c)



(f)

Figure 3. The number of cells on each APC & APC+ Nano-HA pellet 24 h, 72 h and 1 week after seeding determined by MTT assay.

Discussion

Silicate based materials showed promising effects on apatite core formation and the combination with hydroxyapatite crystals were supposed to increase their effects. In this study, the silicate-based cement alone and its combination with Nano-HA particles with diameters of 20-25 nm are compared with each other in terms of adhesion capability with periodontal ligament fibroblast cells and silicate-based cement alone showed superior cellular proliferation. In the term of cell attachment, we

found that there was no statistically significant difference between two groups at 24 h and 1 week. Although there was a significant difference between them at 72 h for the benefit of the Silicate-Based Cement alone group.

The cell population after 24 h reflected initial adhesion on the APC substrates, and a remarkable increase in cell population after 72 h indicated subsequent proliferation of the cells while there was a decline in cell population after 1 week to the level of about the initial adhesion at 24 h. MTT data analysis showed statistically significant

differences between the three time periods. In other words, there was a notable change between 24 h with 72 h and 72 h with 1 week.

On the other hand, the cell population of APC +Nano-HA substrates after 24, 72 h, and 1 week of seeding could reflect initial adhesion on the substrates with no statistically significant difference between three time periods.

Our result for APC medium is in agreement with the study conducted by Abdullah and coworkers (14). In their study cells have been found in close contact with APC (15).

Unexpected result of our study was that the cell population after 1 week of seeding in APC group decreased to the level of about initial seeding at 24 h after a significant rise at 72 h of the seeding. One probable assumption for the inhibition of cell proliferation may be the limitation of the nutrient or the surface area of the substrate necessary for the growth and proliferation in addition to the aggregation of cellular waste products in the *in vitro* study, while in body, blood circulation supplies the nutrients, oxygen, carbon dioxide and hormones and collects the waste materials from cells and transport to lymphatic circulation.

Fibroblast cell adhesion is important for cell division and cell proliferation (16). Typically, cell apoptosis (anoikis) occurs when cells cannot adhere to a scaffold(17) or cannot hold their connection(18). As Okada and others have suggested, reducing the size of the nanoscale unit affects focal adhesion formation, thus influencing the adhesion and proliferation of the cell (19).

Some others have also suggested that the function of fibroblasts is suppressed on the nanostructures (20–22). Okada and others reported that the adhesion and/or proliferation of L929 mouse fibroblasts was restricted on HA nanocrystals smaller than 30 nm (19). However, there are many reports of increased cellular activity in the presence of nanostructures(20–28). Differences in these published articles may be due to the fact that cell function is sensitive to the topography and size of nanostructures. Nanoscale topographic features influence cell behaviors in terms of adhesion, morphology, migration, and proliferation (29, 30). Choi and others, suggested “the needle-like nanostructures should be useful for a biological low adhesive surface, that is, anti-adhesion or antifouling surface” (31). Gao and others (32) reported nano-topographic features to influence the functions of periodontal ligament cells. Therefore, biomaterials for nano-structured scaffolds should be carefully designed taking into account the size and characteristics of cells and substrates.

Subsequent studies should conduct further experiments to better characterize the material, including examining the expression of osteoporosis markers and cementation and comparing it with other mesenchymal stem cells isolated from dental tissues (dental pulp mesenchymal stem cells).

In general, this study revealed that both cement substrates were biocompatible although adding needle shape HA nanoparticles of 20-25 nm to the APC substrate could not enhance fibroblast cell proliferation in one week after seeding.

Conclusions

Although both Nanohydroxyapatite silicate-based cement and silicate-based cement alone are biocompatible, in terms of fibroblast cell attachment, silicate-based cement alone showed superior cellular proliferation in 72 hours. After 24h and 1week both minerals show the same response.

Acknowledgments

The authors appreciate the funding and support for this study provided by the Vice Chancellor of Research Center & Innovation, Shiraz University of Medical Sciences. The Scanning Electron Microscopy (SEM) images for Cellular analysis and TEM data used to support the findings of this study are included within the article.

Conflicts of interests

The authors declare no conflicts of interest.

References

1. Gandolfi MG, Zamparini F, Degli Esposti M, Chiellini F, Aparicio C, Fava F et al. Polylactic acid-based porous scaffolds doped with calcium silicate and dicalcium phosphate dihydrate designed for biomedical application. *Mater Sci Eng C Mater Biol Appl*. 2018; 82:163–181.
2. Prati C, Gandolfi MG. Calcium silicate bioactive cements: Biological perspectives and clinical applications. *Dental Materials*. 2015; 31(4):351–370.
3. Gandolfi MG, Zamparini F, Degli Esposti M, Chiellini F, Fava F, Fabbri P et al. Highly porous polycaprolactone scaffolds doped with calcium silicate and dicalcium phosphate dihydrate designed for bone regeneration. *Materials Science and Engineering C*. 2019; 102:341–361.

4. Khorshidi H, Raofi S, Najafi M, Kalantari MH, Khorshidi Malahmadi J, Derafshi R. Nanohydroxyapatite Silicate-Based Cement Improves the Primary Stability of Dental Implants: An in Vitro Study. *Advances in Materials Science and Engineering* 2017; 2017.
5. Zhao M, Li H, Liu X, Wei J, Ji J, Yang S et al. Response of Human Osteoblast to n-HA/PEEK--Quantitative Proteomic Study of Bio-effects of Nano-Hydroxyapatite Composite. *Sci Rep.* 2016; 6:22832.
6. Ajdary M, Moosavi MA, Rahmati M, Falahati M, Mahboubi M, Mandegary A et al. Health concerns of various nanoparticles: A review of their in vitro and in vivo toxicity. *Nanomaterials.* 2018; 8(9).
7. Chieruzzi M, Pagano S, Moretti S, Pinna R, Milia E, Torre L et al. Nanomaterials for Tissue Engineering In Dentistry. *Nanomaterials.* 2016; 6(7):134.
8. Pepla E, Besharat LK, Palaia G, Tenore G, Migliau G. Nano-hydroxyapatite and its applications in preventive, restorative and regenerative dentistry: a review of literature. *Ann Stomatol (Roma).* 2014; 5(3):108–114.
9. Sadat-Shojai M, Khorasani M-T, Jamshidi A. 3-Dimensional cell-laden nano-hydroxyapatite/protein hydrogels for bone regeneration applications. *Mater Sci Eng C Mater Biol Appl.* 2015; 49:835–843.
10. Wang X, Zhang G, Qi F, Cheng Y, Lu X, Wang L et al. Enhanced bone regeneration using an insulin-loaded nano-hydroxyapatite/collagen/PLGA composite scaffold. *Int J Nanomedicine.* 2018; 13:117–127.
11. Zakaria SM, Sharif Zein SH, Othman MR, Yang F, Jansen JA. Nanophase hydroxyapatite as a biomaterial in advanced hard tissue engineering: a review. *Tissue Eng Part B Rev.* 2013; 19(5):431–441.
12. Venkatesan J, Kim S-K. Nano-hydroxyapatite composite biomaterials for bone tissue engineering--a review. *J Biomed Nanotechnol.* 2014; 10(10):3124–3140.
13. Hayrapetyan A, Bongio M, Leeuwenburgh SCG, Jansen JA, van den Beucken, Jeroen J J P. Effect of Nano-HA/Collagen Composite Hydrogels on Osteogenic Behavior of Mesenchymal Stromal Cells. *Stem Cell Rev.* 2016; 12(3):352–364.
14. Abdullah D, Ford TRP, Papaioannou S, Nicholson J, McDonald F. An evaluation of accelerated Portland cement as a restorative material. *Biomaterials.* 2002; 23(19):4001–4010.
15. Ding S-J, Shie M-Y, Hoshiba T, Kawazoe N, Chen G, Chang H-C. Osteogenic differentiation and immune response of human bone-marrow-derived mesenchymal stem cells on injectable calcium-silicate-based bone grafts. *Tissue Eng Part A.* 2010; 16(7):2343–2354.
16. Ruano R, Jaeger RG, Jaeger MM. Effect of a ceramic and a non-ceramic hydroxyapatite on cell growth and procollagen synthesis of cultured human gingival fibroblasts. *J Periodontol.* 2000; 71(4):540–545.
17. Idogawa M, Adachi M, Minami T, Yasui H, Imai K. Overexpression of BAD preferentially augments anoikis. *Int J Cancer.* 2003; 107(2):215–223.
18. Arnold M, Cavalcanti-Adam EA, Glass R, Blümmel J, Eck W, Kantlehner M et al. Activation of integrin function by nanopatterned adhesive interfaces. *Chemphyschem.* 2004; 5(3):383–388.
19. Okada S, Nagai A, Oaki Y, Komotori J, Imai H. Control of cellular activity of fibroblasts on size-tuned fibrous hydroxyapatite nanocrystals. *Acta Biomater.* 2011; 7(3):1290–1297.
20. Webster TJ, Ergun C, Doremus RH, Siegel RW, Bizios R. Specific proteins mediate enhanced osteoblast adhesion on nanophase ceramics. *J Biomed Mater Res.* 2000; 51(3):475–483.
21. Variola F, Yi J-H, Richert L, Wuest JD, Rosei F, Nanci A. Tailoring the surface properties of Ti6Al4V by controlled chemical oxidation. *Biomaterials.* 2008; 29(10):1285–1298.
22. Kubo K, Tsukimura N, Iwasa F, Ueno T, Saruwatari L, Aita H et al. Cellular behavior on TiO₂ nanonodular structures in a micro-to-nanoscale hierarchy model. *Biomaterials.* 2009; 30(29):5319–5329.
23. Yanagida H, Okada M, Masuda M, Ueki M, Narama I, Kitao S et al. Cell adhesion and tissue response to hydroxyapatite nanocrystal-coated poly(L-lactic acid) fabric. *J Biosci Bioeng.* 2009; 108(3):235–243.
24. Price RL, Ellison K, Haberstroh KM, Webster TJ. Nanometer surface roughness increases select osteoblast adhesion on carbon nanofiber compacts. *J Biomed Mater Res A.* 2004; 70(1):129–138.
25. El-Ghannam AR, Ducheyne P, Risbud M, Adams CS, Shapiro IM, Castner D et al. Model surfaces engineered with nanoscale roughness and RGD tripeptides promote osteoblast activity. *J Biomed Mater Res A.* 2004; 68(4):615–627.

26. Miller DC, Haberstroh KM, Webster TJ. Mechanism(s) of increased vascular cell adhesion on nanostructured poly(lactic-co-glycolic acid) films. *J Biomed Mater Res A*. 2005; 73(4):476–484.
27. Park J, Bauer S, Mark K von der, Schmuki P. Nanosize and vitality: TiO₂ nanotube diameter directs cell fate. *Nano Lett*. 2007; 7(6):1686–1691.
28. Misra SK, Mohn D, Brunner TJ, Stark WJ, Philip SE, Roy I et al. Comparison of nanoscale and microscale bioactive glass on the properties of P(3HB)/Bioglass composites. *Biomaterials*. 2008; 29(12):1750–1761.
29. Flemming RG, Murphy CJ, Abrams GA, Goodman SL, Nealey PF. Effects of synthetic micro- and nano-structured surfaces on cell behavior. *Biomaterials* 1999; 20(6):573–88.
30. Curtis A. Tutorial on the biology of nanotopography. *IEEE Trans Nanobioscience*. 2004; 3(4):293–295.
31. Choi C-H, Hagvall SH, Wu BM, Dunn JCY, Beygui RE, “CJ” Kim C-J. Cell interaction with three-dimensional sharp-tip nanotopography. *Biomaterials*. 2007; 28(9):1672–1679.
32. Gao H, Li B, Zhao L, Jin Y. Influence of nanotopography on periodontal ligament stem cell functions and cell sheet based periodontal regeneration. *Int J Nanomedicine*. 2015; 10:4009–4027.

Corresponding Author

Hooman Khorshidi,

Department of Periodontics, School of Dentistry, Shiraz University of Medical Sciences, Shiraz, Iran

Tell: +98-713-628-0456

Email: khorshidih@sums.ac.ir;